X-Band Isoflux Concentric Circular Antenna Arrays for Image Data Download from LEO Satellites to Ground Stations

M. A. El-Hassan [1], K. F. A. Hussein [1], A. E. Farahat [1], and K. H. Awadalla [2]

[1] Electronics Research Institute (ERI), Cairo, Egypt
mayaboelhassan@yahoo.com, Khalid_elgabaly@yahoo.com, asmaa@eri.sci.eg

[2] Faculty of Electronic Eng., Menoufia University Egypt
kamal_awadalla@hotmail.com

Abstract ─ A circularly polarized isoflux beam synthesized by concentric circular arrays of printed microstrip patch antennas is proposed for X-band transmission of image data from land-imaging LEO satellites to the ground stations. This beam has a wide coverage angle of about 100° of uniform illumination. The paper introduces a novel design of a compact right-hand circularly polarized microstrip patch as an element for the concentric circular arrays. The patch antenna has impedance matching bandwidth of about 600 MHz and axial ratio bandwidth of about 170 MHz at 8.1 GHz. A prototype of the proposed patch antenna is fabricated for experimental measurements. The electromagnetic simulation and experimental results show good agreement. A computationally efficient particle swarm optimization (PSO) procedure is developed and applied to find the distribution of the excitation magnitudes over the array elements so as to generate an isoflux beam in all the elevation planes with circular symmetry in the azimuth planes. The phase of excitation is the same for all the array elements. The method proposed to apply the PSO reduces the computational resources to about 6.5% of those required by the conventional method of application. Moreover, the proposed iterative PSO procedure is shown to be very fast convergent.

Index Terms ─ Concentric circular arrays, isoflux beam, LEO satellite, particle swarm optimization, PSO.

I. INTRODUCTION

A low-earth-orbit (LEO) satellite platform is recommended to radiate a beam with homogeneous power density over the coverage area on the earth surface. For a point on the ground surface just at the satellite nadir the propagation has its minimum value, whereas for off-nadir points, the propagation path is longer. To provide homogeneous power density on the ground, the antenna must compensate the power loss due to the change of the propagation path by increasing the gain toward directions where the path is longer. That is, the antenna gain pattern provides isoflux radiation. An isoflux pattern is omnidirectional (circularly symmetric) with the azimuth angle and has cosecant-squared dependence on the elevation angle. This produces constant signal level at all the points over the beam footprint on the ground surface. It also results in continuous and uniform signal level at the ground station at all the elevation angles during the communication session irrespective of the azimuth direction of the flying vehicle relative to the ground station. For land-imaging LEO satellites using either optical sensor or synthetic aperture radar (SAR), an X-band antenna (or antenna array) is needed for image data transmission from the satellite to the ground stations. As mentioned above, for uniform and continuous reception by the ground station, the satellite antenna should provide isoflux radiation pattern.

The work of [1] introduces the design of sparse concentric circular array to produce isoflux pattern over a visibility cone of about 100° for LEO satellites. In [2] a secant pattern (CP) antenna is designed by combining a CP generating adaptor and a secant pattern radiator. In [3] an isoflux pattern presented by a compact X-band antenna with circularly polarized for a nanosatellite platform that imposes an important volume constraint. In [4] a microstrip phased array is designed and optimized using genetic algorithm to produce isoflux pattern by two concentric ring arrays for operation in the X-band with application to LEO cubesat communications. In [5] the design of concentric ring arrays for isoflux radiation is presented, with considering the reduction of the sidelobe level for medium earth orbit (MEO) satellite using particle swarm optimization (PSO) technique. In [6], a design of a patch antenna array is introduced for a reconfigurable isoflux pattern, with fewer levels of excitations to diminish the hardware complexity using PSO and harmony search algorithm (HSA) as optimization approach. In [7], a design of concentric ring antenna arrays for isoflux radiation for geostationary earth orbit (GEO) and MEO satellites is performed using

Submitted On: May 28, 2019
Accepted On: September 7, 2019

an evolutionary multi-objective optimization technique. In [8], a phase-only synthesis algorithm is applied to design lens-array antennas to produce flat-topped and isoflux beams.

The PSO algorithm is commonly used to optimize antenna arrays to synthesize beam shapes required for various applications [9]. In this paper, a planar array of concentric circular arrays of circularly polarized microstrip patch antennas is optimized to produce circularly symmetric isoflux beam using the PSO technique. A novel X-band circularly polarized microstrip patch antenna with corner slots is designed to be the element of the proposed array. A prototype of the proposed patch antenna is fabricated for experimental measurement of the impedance matching bandwidth and the radiation patterns of the circularly polarized fields. The PSO is applied to optimize the magnitudes of excitation of the radiating elements which are arranged in 5 coplanar circular arrays with a total number of 93 elements. The magnitudes of excitation for all the elements on the same circle are kept equal to each other. Thus, the magnitudes only are allowed to vary in the radial direction to achieve the optimization goals. The numerical results of the present work are concerned with the application of the PSO to concentric circular arrays of isotropic point sources and as well as concentric circular arrays of printed microstrip patches. The presentation and discussions of the numerical results focus on the investigation of the performance of the single element as well as the optimized array. The commercially available package CST® is used for electromagnetic simulation for the purpose of ensuring the correctness and accuracy of the obtained results.

The major improvements can be addressed in the present work: (i) the reduction of computational cost (time and memory space) of the PSO algorithm, and (ii) the fast convergence of the iterative procedure to arrive at the required beam shape.

II. BEAM SHAPE FOR ISOFLUX RADIATION FROM LEO SATELLITES

A spherical model for the earth and, hence, a circular path of the satellite around the earth can be assumed as shown in Fig. 1. The function $R_s(\theta)$ indicates the relative distance of the satellite to any point of the illuminated earth surface in any cut of the azimuth plane, h represents the height of the satellite, an a_E is the equatorial radius of the earth.

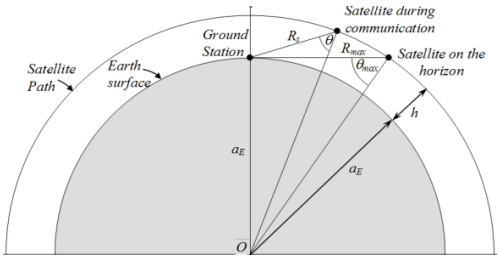

Fig. 1. Low-earth-orbit satellite path about the earth during a communication session with the ground station.

It is assumed that the communication session between the satellite and the ground station can start as soon as the satellite appears to the ground station just on the horizon and ends when the satellite disappears below the horizon. Practically, the communication session does not start unless the satellite reaches a minimum elevation angle, θ_{min}, above the horizon and ends just when the satellite elevation angle becomes lower than this value. During the communication session, the communication range R_s (the distance between the satellite and the ground station) changes according to the following relation:

$$R_s(\theta) = (h + a_E)\cos\theta - \sqrt{(h + a_E)^2\cos^2\theta - h(h + 2a_E)}\,. \quad (1)$$

To keep the power density at the ground station at a fixed level irrespective of the satellite position during the communication session, the power radiated from such an antenna should be proportional to the square of the communication range.

According to the above discussion, for a LEO satellite orbiting the earth at an altitude of 1000 km, the working sector of the main lobe of the radiation pattern should be $\approx 100° \times 100°$. The directional pattern shape, within the limits of its working sector, should be conical and close to a funnel shape, with directions of maximum radiation at angles of about $\pm 50°$ from nadir.

Thus, to provide uniform power density over the coverage area on the ground, the antenna must compensate the power loss due to the propagation path by raising the gain toward directions where the path is longer. According to the description of the isoflux pattern in the coverage sector of the radiation pattern the antenna gain should meet the requirement determined by the following expression:

$$G(\theta) = G_{max}\left(\frac{R_S(\theta)}{R_{max}}\right)^2, \quad (2)$$

where $R_{max} = 2610$ km is the maximum distance between antenna and ground station at an orbital altitude of 1000 km, θ is the observation angle versus the direction of the Earth center and elevation angle of the satellite 5°. In this case, the gain of the antenna in the directions of the maximum radiation should be about 6 dBi.

III. BEAM SHAPING USING CONCENTRIC CIRCULAR ARRAYS

Two degrees of freedom are required for the control parameters to get isoflux three-dimensional beam for uniform radiation over a given solid angle. The circularly symmetric distribution with the azimuth angle and the uniform distribution with the elevation angle require concentric circular arrays like those shown in Fig. 2. Each circular array has a number of elements proportional to its radius so as to keep equal circumferential distances between the contiguous elements on the circles. The distribution of excitation magnitudes with radial direction controls the beam shape with the elevation angle whereas the magnitudes distribution with the circumferential dimension controls the beam shape with the azimuth angle. A central element may be added to the concentric circular array. As discussed in [10] adding a central element to a circular array improves the array gain and reduces the sidelobe level.

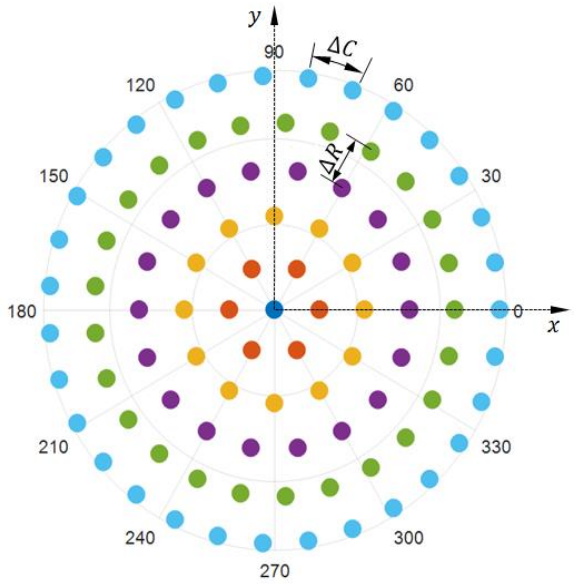

Fig. 2. Concentric circular arrays with growing size for synthesized isoflux beams with circular symmetry.

A. Radiation pattern of concentric circular arrays

For a circular array of isotropic point source radiators and that all the elements have the same phase of excitation, the radiation pattern can be calculated as follows:

$$E(\theta,\phi) = \sum_{n=1}^{N_P} A_n \, e^{jk_o R \sin\theta \cos(\phi-\Phi_n)}, \quad (3)$$

where R is the radius of the circle, $R = N_P \Delta C/2\pi$, ΔC is the inter-element arc spacing, Φ_n is the angular position of n^{th} element in the $x-y$ plane, $\Phi_n = 2n\pi/N_P$ with $1 \le n \le N_P$, ϕ is the azimuth angle measured with the positive x-axis, θ is the elevation angle measured with the positive z-axis, k_0 is the free space wave number, $k_0 = 2\pi/\lambda_0$, λ_0 is the wave length in free space, A_n is the excitation coefficient (amplitude and phase) of the n^{th} element. It can be written as $A_n = I_n \, e^{j\alpha_n}$ where, $I_n =$ excitation amplitude of the n^{th} element and α_n is the phase excitation of the n^{th} element (relative to the array center).

Let the antenna array be arranged as N_R concentric circular arrays with a growing number of elements. Assume that the radii of the concentric circles are uniformly increasing; this means that the radius of the circle number m, $(m = 1,2,..,N_R)$ is $R_m = m\,\Delta R$. The arrangement of the elements of such concentric circular array is shown in Fig. 2. On the m^{th} circle, a number of $N_P(m)$ elements are uniformly arranged over the circle circumference. The circumferential distance between the contiguous elements on the m^{th} circle can be expressed as follows:

$$\Delta C \equiv \Delta P_m = \Delta\Phi R_m = \frac{2\pi R_m}{N_P(m)} = \frac{2\pi m}{N_P(m)}\Delta R \, . \quad (4)$$

The following expression can be used to calculate $N_P(m)$,

$$N_P(m) = \text{round}\,(2\pi\, m). \quad (5)$$

According to this equation, irrespective of the value of m, the separation ΔP_m for all the circles is kept as near as possible to ΔR. Also, this equation indicates that the minimum number of elements on one circle is 6.

An extra element is located at the center of the entire array. The coefficient of the excitation voltage of the n^{th} element on the m^{th} circle is $A_{m,n}$. The coefficient of excitation of the central element is A_0.

Assuming that the elements are isotropic point source radiators and that all the elements have the same phase of excitation, the radiation pattern can be calculated as follows:

$$E(\theta,\phi) = A_0 + \sum_{m=1}^{N_R}\sum_{n=1}^{N_P(m)} A_{m,n} \, e^{jkR_m \sin\theta \cos(\phi-\Phi_{m,n})}, \quad (6)$$

where, $\Phi_{m,n}$ is the angular position (with the positive x-axis) of the n^{th} array element on the m^{th} circular array, $\Phi_{m,n} = 2\pi n/N_P(m)$; $m = 1, \ldots, N_R$, $n = 1, 2, \ldots, N_P(m)$.

B. Concentric circular arrays for circularly symmetric radiation pattern

To enforce circular symmetry of the synthesized radiation pattern, all the elements on the same circle must have the same magnitude of excitation; this means,

$$A_{m,n} = A_m, \; m = 1,2,\ldots,N_R, \; n = 1,2,\ldots,N_P(m). \quad (7)$$

Substituting from (7) into (6), the following expression

is obtained for the radiated field in the far zone,

$$E(\theta,\phi) = A_0 + \sum_{m=1}^{N_R}\Big(A_m \sum_{n=1}^{N_P(m)} e^{jkR_m \sin\theta\cos(\phi-\Phi_{m,n})}\Big). \quad (8)$$

C. Application of the particle swarm optimization for shaping the beam of concentric circular arrays

The PSO technique achieves the required optimization by setting the positions of each individual particle within a moving swarm so as to get the overall swarm as near as possible to a predetermined goal. The algorithm developed to implement the PSO should have its goal to minimize a predefined cost function. The latter expresses the distance to a required electromagnetic objective. The movements and interactions of the particles within the swarm are considered during the calculation of the improved positions that make the overall swarm approaches the required goal. In the problem of beam shaping by an antenna array, each particle position represents a possible set of magnitudes of the feed of the elements of the array, i.e., it represents one point in the optimization space. The implementation of the PSO algorithm can be divided into four stages: (i) initialization of positions, $\mathbf{x}_n^{(0)}$ and velocities, $\mathbf{v}_n^{(0)}$, for the particles of the swarm, (ii) calculation of the local best positions, $\mathbf{y}_n$, for the particles, (iii) Calculation of the global best position, $\mathbf{g}$, (iv) Calculation of the particles velocities, $\mathbf{v}_n^{(1)}$, and positions, $\mathbf{x}_n^{(1)}$, for the next iteration[11].

The following equations are used to implement an iterative PSO algorithm:

$$\mathbf{v}_n^{(t)} = w\,\mathbf{v}_n^{(t-1)} + c_1 r_1\big(\mathbf{y}_n^{(t-1)} - \mathbf{x}_n^{(t-1)}\big) + c_2 r_2\big(\mathbf{g}^{(t-1)} - \mathbf{x}_n^{(t-1)}\big), \quad (9)$$

$$\mathbf{x}_n^{(t)} = \mathbf{x}_n^{(t-1)} + \mathbf{v}_n^{(t)}, \quad (10)$$

where t is the iteration number (time index) and n is the particle number. For each particle, the initial position, $\mathbf{x}_n^{(0)}$, is determined by assigning random values (varying around the unity) to the amplitudes of the excitation voltages of the array elements. The initial local best position of each particle, $\mathbf{y}_n^{(0)}$, is assigned the same initial value of the particle position. The initial value of the velocity of each particle is set to zero. The local best position, $\mathbf{y}_n$, for each particle is the position of this particle that results in the minimum value of the cost function over the successive iterations during the run of the PSO algorithm. The global best position, $\mathbf{g}$, for the particles in the swarm is the position among the local best positions that results in the absolute minimum value of the cost function over the successive iterations during the run of the PSO algorithm. In each iteration, the velocity, $\mathbf{v}_n$, and position, $\mathbf{x}_n$, for each particle in the swarm are updated, as given by (9) and (10).

D. Computational improvement of the PSO algorithm

The PSO algorithm is applied to get the optimum values of only 6 magnitudes of excitation; one for all the elements in each circular array plus the central element. In this way, each particle in the swarm has its position as one-dimensional vector with only 6 real elements, which can be expressed as follows:

$$\mathbf{x}_n^{(t)} = \begin{pmatrix} A_0^{(t)} & A_1^{(t)} & A_2^{(t)} & A_3^{(t)} & A_4^{(t)} & A_5^{(t)} \end{pmatrix}^T. \quad (11)$$

Thus, instead of applying the PSO to find 93 optimum positions (the total number of the array elements) it is applied only to find 6 optimum positions (the number of concentric circular arrays). This can be considered a major improvement that considerably reduces the computational complexity of the PSO algorithm. As the swarm has 15 particles whose positions should be calculated in each iteration of the PSO algorithm, the total number of the values that should calculated in each iteration are reduced to 90 values (15 × 6) instead of 1395 values (15 × 93). As the PSO algorithm runs for about 150 iterations to arrive at accurate results, the reduction ratio of the computational time is (1395-90)/1395×100% = 93.5%. Similarly, the required memory space is reduced by the same percentage (93.5%).

The main objective of the PSO algorithm is to realize the target beam shape described by $\hat{E}(\theta)$. From (1) and (2) one can deduce the desired isoflux radiation pattern to achieve uniform distribution of the power density over the satellite footprint. This means that the desired electric field radiation pattern should take the form given by the following expression:

$$E_d(\theta) = \frac{R_s(\theta)}{R_{max}} = E_o\left[\frac{(h+a_E)\cos\theta}{-\sqrt{(h+a_E)^2\cos^2\theta - h(h+2a_E)}}\right], \quad (12)$$

where, E_o is the constant magnitude of the radiated electric field in the far zone. Thus, the target beam shape for the PSO algorithm can be defined as follows:

$$\hat{E}(\theta) = \begin{cases} E_d(\theta), & 0 < \theta \le \frac{1}{2}\Theta_a,\ 0 < \phi < 2\pi \\ 0, & \frac{1}{2}\Theta_a < \theta < \pi,\ 0 < \phi < 2\pi \end{cases}, \quad (13)$$

where Θ_a is the desired beam width.

As the main goal of the PSO during its iterations is to reduce the cost function, the latter should be increased as the achieved radiation pattern further deviates from the ideal pattern. Thus, the cost function can be, simply, the absolute difference between the achieved and the desired (ideal) patterns of the electric field as follows:

$$F_C = W_F\big(\big|E - \hat{E}\big|\big) + W_S\big(\big|E - \hat{E}\big|\big), \quad (14)$$

where W_F is a weighting coefficient of the part of the cost function ensuring the required beam shape over the illuminated angular zone defined by: $0 < \theta \le \frac{1}{2}\Theta_a$, W_S is a weighting coefficient for the part of the cost function

ensuring cancelation of the sidelobes over the angular zone: $\frac{1}{2}\Theta_a < \theta < \pi$.

In conclusion, the amplitudes and phases of the elements of different circles to satisfy the performance goal by the PSO algorithm so as to satisfy the required beam shape and the remaining objectives of the antenna array design such as the axial ratio and the sidelobe level.

IV. CORNER-SLOTTED MICROSTRIP PATCH ANTENNA FOR CIRCULAR POLARIZATION

This section presents a brief description of the circularly polarized microstrip patch antenna proposed for the implementation of the concentric circular array to produce the isoflux beam. The circular polarization is obtained from a square microstrip antenna by etching two symmetric L-shaped slots near two diagonally facing corners of the square patch as shown in Fig. 3. Right-hand circular polarization (RHCP) is obtained if one slot is cut near the right upper corner and the other slot is cut near the left lower corner as shown in Fig. 3. In analogous manner, LHCP is obtained if one slot is cut at the left upper corner and the other slot is cut at the right lower corner. The patch is square of side length L_P and has four side slots and two corner slots. A corner slot is L-shaped and has two arms; each of length L_{CS} and width W_{CS}. The separation between the slot edge and the patch edge is t_S. The four side slots are cut along the horizontal and vertical axes of symmetry and proposed to enhance circular polarization and make the antenna size compact. Each of the four side slots has a length of L_s and a width of W_s. The lengths of the slots and the position of the feed are set to obtain good impedance matching and to produce acceptable value of the axial ratio over the radiation zone of interest. The ground plane is square with side length G. The feeding probe is located at a distance F from the patch center $(x = 0, y = F)$ as shown in Fig. 3.

V. RESULTS AND DISCUSSIONS

A planar concentric circular array with an inter-radial spacing of 0.5λ is optimized to produce isoflux beam. The array is arranged in the x-y plane and is composed of 5 coplanar circular arrays with a total number of 93 elements, where 92 elements are distributed in the 5 circles and an extra element is located at the center of the array. The elements on each circle are equispaced along its perimeter. The number of elements on the five circles arranged from the innermost to the outermost are 6, 12, 18, 25, 31, and the radii of the circles are $\lambda/2, \lambda, 3\lambda/2, 2\lambda, 5\lambda/2$, respectively.

The PSO algorithm is applied to produce an isoflux beam from such concentric circular arrays as explained in Section 2, where the working parameters of the PSO are set as follows: the swarm size (number of particles) is $p = 15$, the inertia coefficient, $w = 0.729$, the maximal velocity, $\mathbf{v}_{max} = 0.2$, the cognitive rate coefficient $c_1 = 1.0$, the social rate coefficient $c_2 = 2.0$. The PSO algorithm runs for 150 iterations.

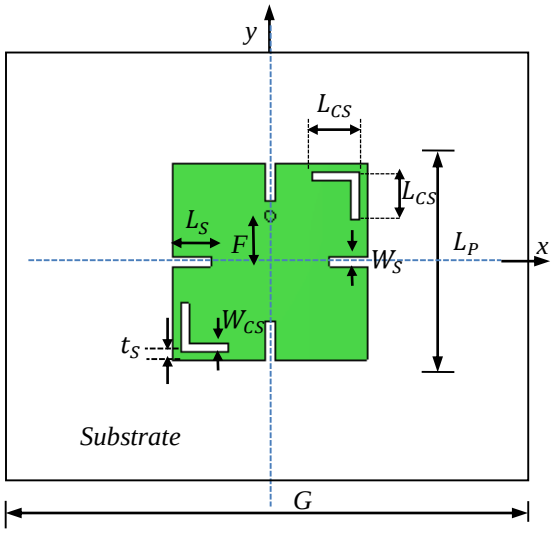

Fig. 3. The proposed compact circularly polarized corner-slotted patch antenna.

A. Assessment of the circularly polarized corner-slotted microstrip patch

The optimal design parameters of the patch antenna to produce RHCP are $L_P = 7.5$ mm, $G = 20.6$ mm, $L_s = 1.1$ mm, $L_{SC} = 1.6$ mm, $W_s = 0.36$ mm, $W_{SC} = 0.27$ mm, $t_S = 0.28$ mm, and $F = 1.6$ mm. It should be noted that in the following presentation and discussions of the numerical results the patch antenna has the same design parameters listed above unless otherwise indicated. The patch is printed on a roger TMM4 substrate with permittivity $\varepsilon_r = 4.5$, loss tangent $\delta = 0.002$, and thickness $h = 1.524$ mm.

A prototype of a single patch antenna is fabricated in the laboratory for experimental verification of the simulation results concerning the dependence of the reflection coefficient on the frequency and the radiation patterns of the circularly polarized fields. Top and bottom views of the fabricated antenna are presented in Fig. 4. The vector network analyzer of the Agilent Field Fox N9918A is used to measure S_{11} at the antenna port against the frequency. Figure 5 shows the experimental setup with the fabricated prototype of the proposed antenna. The results for the dependence of S_{11} on the frequency are plotted and presented in Fig. 6, where the comparison between the experimental and simulation results of the reflection coefficient shows good agreement. The simulation results for S_{11} show that the patch antenna has an impedance matching bandwidth of about 600MHz (7.81 – 8.42 GHz) for reflection

coefficient < - 10 dB. In the same figure the axial ratio is plotted against the frequency with a minimum axial ratio of about 0.12 dB and a 3 dB axial ratio bandwidth of about 170 MHz (8.02 – 8.19 GHz), with a maximum gain of about 6.4 dBi.

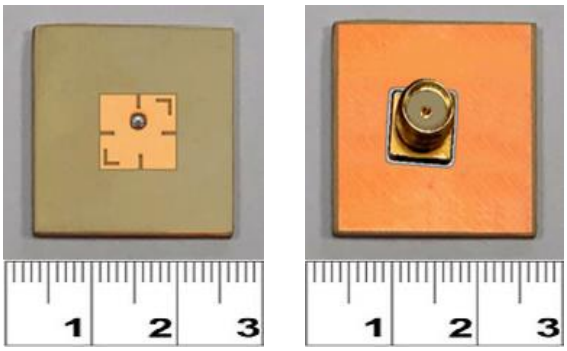

(a) Top view (b) Bottom view

Fig. 4. A fabricated prototype of the circularly polarized patch antenna.

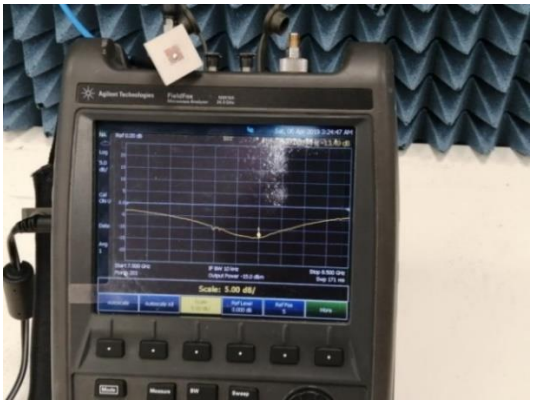

Fig. 5. Experimental measurements of S_{11} for the circularly polarized patch antenna using vector network analyzer of the Agilent Field Fox N9918A.

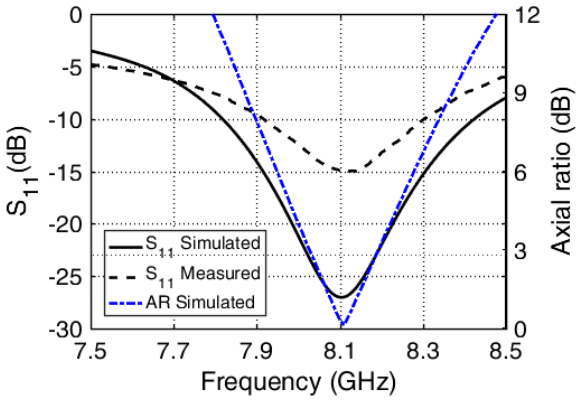

Fig. 6. Frequency dependence of S_{11} and the axial ratio for the circularly polarized patch antenna.

For experimental measurement of the RHCP radiation pattern, the dual circularly polarized antenna model JXTXLB-OSJ-20180 is used as a reference antenna and the experimental setup is made as shown in Fig. 7. The radiation patterns are measured at 8.1 GHz in the two principal planes $x-z$ ($\phi = 0°$) and $y-z$ ($\phi = 90°$). The radiation patterns obtained through simulation and experimental measurements are presented in Fig. 8 showing good agreement. It seems that the radiation is dominated by right-hand circularly polarized electric field component.

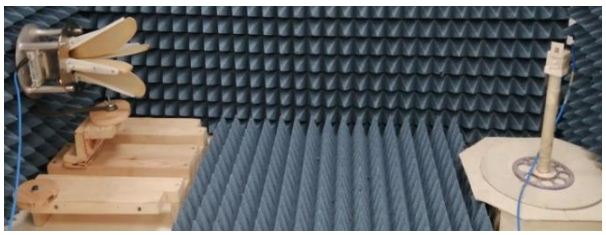

Fig. 7. Experimental setup for measurement of the antenna radiation patterns.

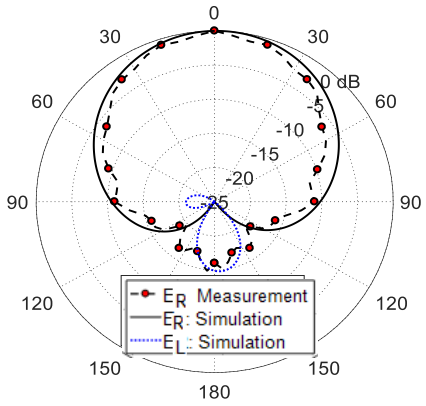

(a) Radiation pattern in the plane $\phi = 0°$

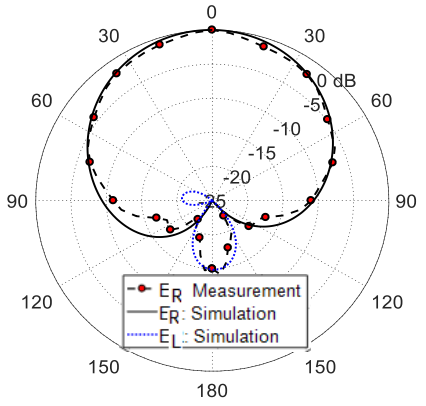

(b) Radiation pattern in the plane $\phi = 90°$

Fig. 8. Radiation patterns for the circularly polarized fields radiated by the microstrip patch.

The directional patterns for the axial ratio produced by the circularly polarized patch antenna are plotted with θ and ϕ as shown in Figs. 9 (a)-(b), respectively, at 8.1 GHz. The 3 dB axial ratio beam width is about 188° $(-123°\ to + 65°)$ in the plane $\phi = 0°$ and is about 162° $(-94\ °to + 68°)$ in the plane $\phi = 90°$. For the elevation angles $\theta = 10°,\ 20°,\ 30°,\ 40°, 50°$ the axial ratio is maintained below 3dB for all the values of ϕ.

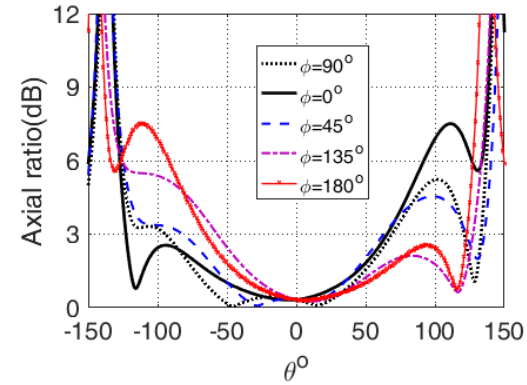

(a) Variation of the axial ratio with θ

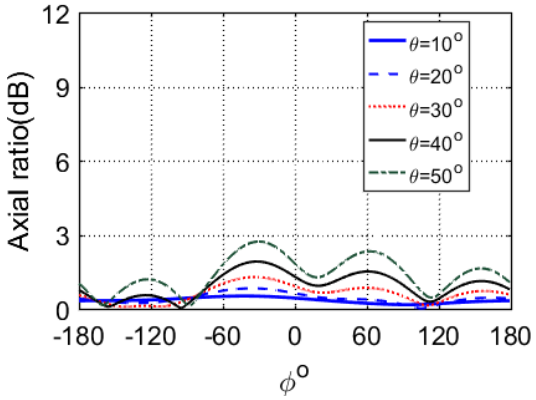

(b) Variation of the axial ratio with ϕ

Fig. 9. Radiation pattern for the axial ratio of the patch antenna at frequency 8.1 GHz.

Table 1: Arrangement of the radiating elements in a concentric circular array with the magnitudes of excitation to produce isoflux beam

Circle Number	0	1	2	3	4	5
Number of Elements	1	6	12	18	25	31
Radius	0	ΔR	2 ΔR	3 ΔR	4 ΔR	5 ΔR
Magnitudes	1.297	2.509	-1.460	0.282	0.358	-0.245

B. Isoflux beam synthesized using concentric circular arrays of point source elements

The PSO is applied to produce isoflux beam by the concentric circular array that is arranged as described in Section III. In the present section the radiating elements of this array are taken as isotropic point sources. During the optimization procedure, all the array elements are kept in-phase. In the meantime, the magnitudes of excitation for all the elements on the same circle are kept equal to each other. Thus, the magnitudes only are allowed to vary in the radial direction to achieve the optimization goals. The optimization procedure aims to find the radial distribution of the excitation magnitudes so as to generate an isoflux beam in all the elevation planes. Consequently, the produced beam will be circularly symmetric and independent of ϕ.

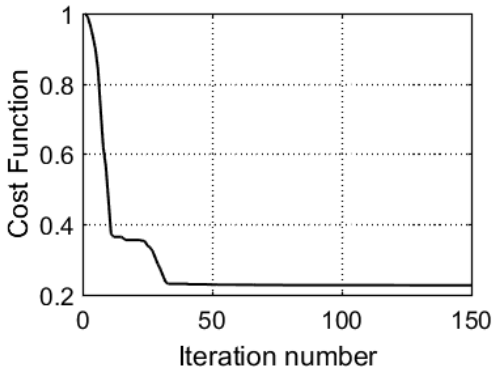

(a)

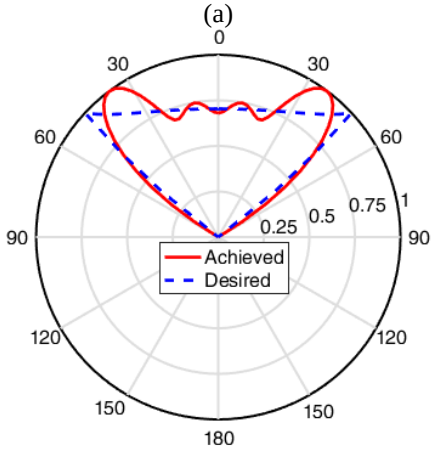

(b)

Fig. 10. The isoflux beam obtained from the application of the PSO algorithm on a concentric circular array of 92 elements arranged on 5 concentric circles plus a central element: (a) decay of the cost function while preceding with iterations, and (b) the achieved isoflux beam in the elevation plane compared with the desired one.

To produce an isoflux beam of width 100°, the excitation magnitudes of the central element and the other concentric circles are listed in Table 1. The cost function with the successive iterations of the PSO algorithm is presented in Fig. 10 (a). It is clear that the algorithm is rapidly convergent as it takes less than 70 iterations to reach a good steady state value of the cost function (about 20% of its initial value). Such fast

convergence and low value of the cost function reflect the efficiency of the applied PSO algorithm. The normalized pattern achieved by the PSO algorithm in the elevation plane (i.e., with θ) is presented in Fig. 10 (b) and compared with the desired one. The desired and achieved three-dimensional radiation patterns are presented in Figs. 11 (a)-(b), respectively. Both the polar plots and the three-dimensional plots presented in Figs. 10 and 11, respectively show satisfactory agreement between the desired beam shape and that achieved using the PSO algorithm.

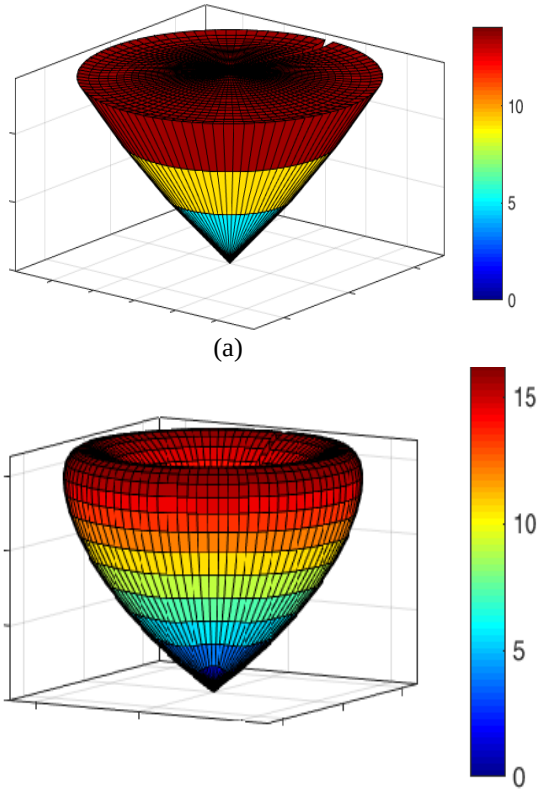

(a)

(b)

Fig. 11. 3D isoflux radiation pattern obtained by concentric circular arrays of 92 elements arranged in 5 circles plus a central element: (a) desired beam shape, and (b) achieved beam shape.

C. Circularly-polarized isoflux beam synthesized by concentric circular arrays of corner-slotted microstrip patches

To produce an isoflux beam with circular polarization, the array element should be circularly polarized. For practical considerations, it is recommended that the concentric circular array be implemented as an array of printed elements. For this purpose, the circularly polarized microstrip patch antenna described in Section IV is proposed as an element for this array. This can be considered a practical and cost-effective implementation of the concentric circular arrays with the same distribution of the excitation magnitudes obtained for the hypothetical point source array described in Section V, B. A planar array composed of concentric circular arrays of 93 elements of such type of patches is proposed to produce the isoflux beam. The dimensions of such a planar array are 210 mm × 210 mm and, hence, it has the advantages of low profile, lightweight, and eases of manufacturing using printed circuit techniques. The 93 patch elements of the array are excited in phase with the magnitudes listed in Table 1. The achieved radiation patterns in the elevation planes $\phi = 0°$ and $\phi = 90°$ at 8.1 GHz are presented in Fig. 12.

The frequency dependence of the axial ratio of the optimized beam in the forward direction ($\theta = 0°$) is presented in Fig. 13. It is clear that the band width for axial ratio < 3dB is about 100 MHz (8.03- 8.13 GHz); whereas for axial ratio < 6dB, the bandwidth is about 260 MHz (7.94 - 8.2 GHz).

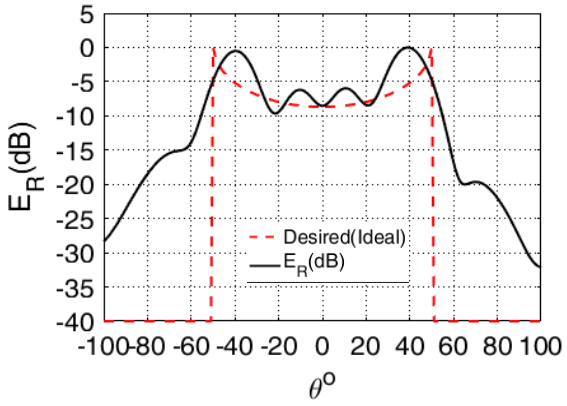

(a) Plane $\phi = 0°$

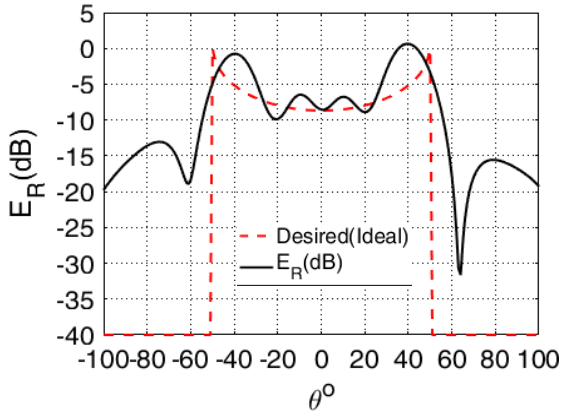

(b) Plane $\phi = 90°$

Fig. 12. The isoflux beam achieved using a 93-element concentric circular array of circularly polarized patch antennas compared with the desired shape, $f = 8.1$ GHz.

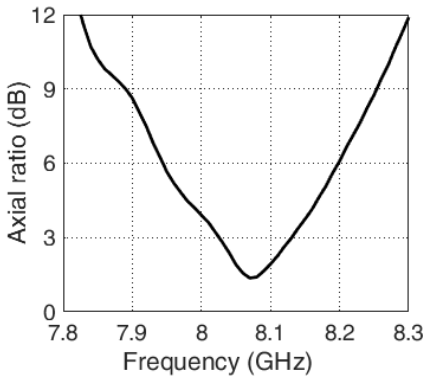

Fig. 13. Axial ratio in the forward direction ($\theta = 0°$) versus frequency for an isoflux beam produced by concentric circular arrays of circularly polarized patches, f = 8.1 GHz.

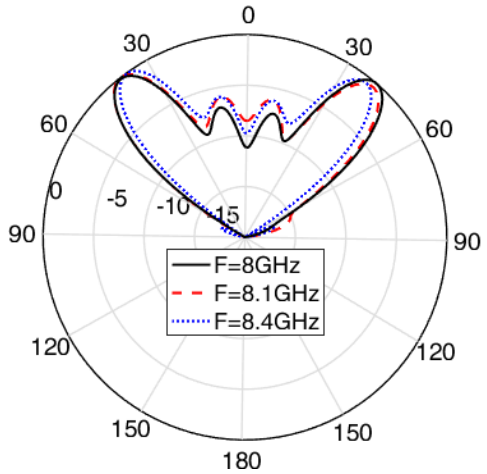

(a) Plane $\phi = 0°$

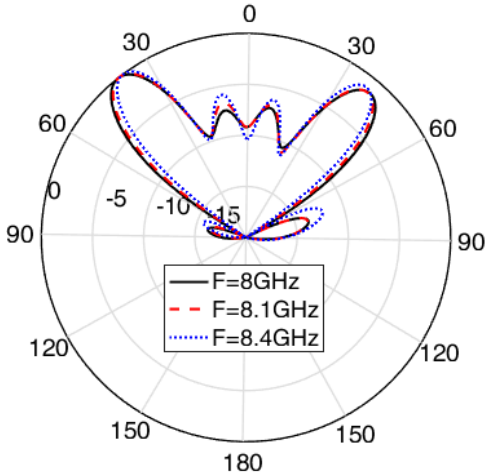

(b) Plane $\phi = 90°$

Fig. 14. Polar plots of the isoflux beam produced by concentric circular arrays of circularly polarized patch antennas at different frequencies in the elevation planes: (a) $\phi = 0°$, and (b) $\phi = 90°$.

Polar plots of the isoflux beam achieved using the concentric circular arrays described above are presented in Fig. 14 at the frequencies 8, 8.1, and 8.4 GHz. As shown in the figure, the isoflux beam is achieved over a frequency band of about 600 MHz (7.8 - 8.4 GHz) with acceptable accuracy of the beam shape.

A three-dimensional plot of the radiation pattern achieved by the concentric circular arrays described above is presented in Fig. 15. It is clear that the beam produces isoflux radiation in the elevation planes with circular symmetry in the azimuth plane.

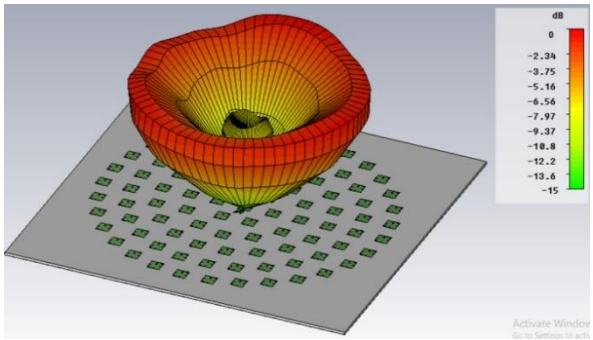

Fig. 15. Three-dimensional plot of the isoflux radiation pattern produced by optimized concentric circular arrays of circularly polarized patch antennas, *f* = 8.1 GHz.

VI. CONCLUSION

A planar array composed of concentric circular arrays of printed microstrip antennas is optimized to synthesize an isoflux beam for X-band transmission of image data from land imaging LEO satellites to the ground stations. A compact right-hand circularly polarized microstrip patch is designed to be an element of the concentric circular arrays. Both simulation and experimental results show that the impedance matching bandwidth of the proposed microstrip patch antenna is about 600 MHz, whereas the axial ratio bandwidth is about 170 MHz at 8.1 GHz. The radiation patterns for the circularly polarized fields are obtained through electromagnetic simulation and experimental measurement showing good agreement. The PSO is applied to find the magnitudes of excitation for the array elements, while keeping the phases equal, so as to synthesize an isoflux beam with circular symmetry. The proposed application method of the PSO is shown to be computationally efficient as it reduces the required computational resources to about 6.5% of those required by the conventional method. The iterative PSO procedure is shown to have fast convergence to arrive at the optimization goals.

REFERENCES

[1] M. Ibarra, M. A. Panduro, Á. G. Andrade, and A. Reyna, “Design of sparse concentric rings array for

LEO satellites," *Journal of Electromagnetic Waves and Applications*, vol. 29, no. 15, pp. 1983-2001, 2015.

[2] J. M. Yim, J. K. Son, T. K. Lee, J. W. Lee, and W. K Lee, "Secant pattern radiator for X-band data transmission," *Asia-Pacific Microwave Conference Proceedings* (*APMC), IEEE*, pp. 1178-1180, 2013.

[3] R. Manrique, G. Le Fur, N. Adnet, L. Duchesne, J. M. Baracco, and K. Elis, "Telemetry X-band antenna payload for nano-satellites," In *11th European Conference on Antennas and Propagation* (*EUCAP), IEEE*, pp. 549-552, Mar. 2017.

[4] J. E. Diener, R. D. Jones, and A. Z. Elsherbeni, "Isoflux phased array design for cubesats," *IEEE APS Conference*, pp. 1811-1812, 2017.

[5] A. R. Maldonado, M. A. Panduro, and C. del Rio-Bocio, "On the design of concentric ring arrays for isoflux radiation in MEO satellites based on PSO," *Progress In Electromagnetics Research*, vol. 20, pp. 243-255, 2011.

[6] A. R. Maldonado, M. A. Panduro, C. del Rio Bocio, and A. L. Mendez, "Design of concentric ring antenna array for a reconfigurable isoflux pattern," *Journal of Electromagnetic Waves and Applications*, vol. 27, no. 12, pp. 1483-1495, 2013.

[7] M. Ibarra, M. A. Panduro, and A. G. Andrade, "Differential evolution multi-objective for optimization of isoflux antenna arrays," *IETE Technical Review*, vol. 33, no. 2, pp. 105-114, 2016.

[8] S. Loredo, G. Leon, O. F. Robledo, and E. G. Plaza, "Phase-only synthesis algorithm for transmitarrays and dielectric lenses," *ACES Journal*, vol. 33, no. 3, 2018.

[9] W.-C. Weng, "Optimal design of an ultra-wideband antenna with the irregular shape on radiator using particle swarm optimization," *Applied Computational Electromagnetics Society Journal (ACES) Journal*, vol. 27, no. 5, 2012.

[10] D. Mandal, K. Kola, J. Tewary, V. Roy, and A. Bhattacharjee, "Synthesis of steered flat-top beam pattern using evolutionary algorithm," *Advanced Electromagnetics*, vol. 5, no. 3, pp. 86-90, 2016.

[11] M. A. El-Hassan, K. F. A. Hussein, and K. H. Awadalla, "Shaped beam circularly polarized circular array for SAR and satellite applications," 36th *National Radio Science Conference* (*NRSC 2019*), *AASTMT*, Port Said, Egypt, B2, Apr. 16-18, 2019.